ADVANCED FUNCTIONAL MATERIALS
www.afm-journal.de

Self-Powered Trace Memorization by Conjunction of Contact-Electrification and Ferroelectricity

*Xiangyu Chen, Mitsumasa Iwamoto, Zhemin Shi, Limin Zhang, and Zhong Lin Wang**

Triboelectric nanogenerator (TENG) is a newly invented technology that can effectively harvest ambient mechanical energy from various motions with promising applications in portable electronics, self-powered sensor networks, etc. Here, by coupling TENG and a thin film of ferroelectric polymer, a new application is designed for TENG as a self-powered memory system for recording a mechanical displacement/trace. The output voltage produced by the TENG during motion can polarize the dipole moments in the ferroelectric thin film. Later, by applying a displacement current measurement to detect the polarization density in the ferroelectric film, the motion information of the TENG can be directly read. The sliding TENG and the single-electrode TENG matrix are both utilized for realizing the memorization of the motion trace in one-dimensional and two-dimensional space, respectively. Currently, the ferroelectric thin film with a size of 3.1 mm^2 can record a minimum area changing of 30 mm^2 and such resolution can still be possibly improved. These results prove that the ferroelectric polymer is an effective memory material to work together with TENG and thereby the fabricated memory system can potentially be used as a self-powered displacement monitor.

1. Introduction

Recently, triboelectric nanogenerators (TENG) by coupling triboelectric effect and electrostatic induction have been intensively developed to be a new method for converting mechanical energy in our daily life into electric power.[1,2] TENG is a new kind of energy harvesting technique and it has unique working principle, which can be adapted to many dynamic systems. Accordingly, TENGs with various structures have been designed for a wide variety of energy harvesting applications, including motion energy harvesting, raindrop energy collection, wind energy gathering, and so on.[3–5] Meanwhile, by utilizing the universal availability of tribo-electricity, this energy generation technique was also applied for designing various self-powered sensor devices, such as motion detectors, skin sensor, liquid sensor, and so on.[6–8] Generally speaking, the mainstreams of the research for TENG are developing into two paths. One is related to the enhancement of the power generation from TENG.[9,10] A common characteristic of the TENG is a high output voltage (hundreds of volts) but low output current. It is therefore necessary to increase charge separation cycles within the limited time in order to improve the charge transfer rate through the devices, which is the current. In addition to high efficiency, another research direction of TENG is to enrich its functionality as self-powered devices. As a result, a series of sensor devices as well as several hybrid power systems based on the concept of tribo-electrification are designed and applied for various purposes.[11,12] Consequently, in order to further popularize the practical utilization of TENG as a low-cost and sustainable new energy technology, it is quite necessary to keep developing some novel and functional applications for TENG technique.

On the other hand, polymer Poly(vinylidene fluoride-trifluoroethylene) (P(VDF-TrFE))[13–15] is a kind of ferroelectric material that has been widely studied for organic memory devices, where two different orientations of dipole moments (up and down) can be briefly considered as "0" and "1" signal for computation and information storage. The dipole moment in P(VDF-TrFE) also can modulate the distribution of local electric field in the organic active layer, which makes a great contribution to enhance charge separation and transport in the organic electronics devices.[16,17] The spontaneous polarization of the P(VDF-TrFE) is very sensitive to the applied electric field and less depending on the conduction current, which is very suitable for the TENG's output characteristic of high voltage and low current. Meanwhile, the dipole switching time of such materials is less than millisecond, which is also compatible for the motion of TENG. Furthermore, it has been found that the ferroelectric performance of P(VDF-TrFE) remains unchanged until for more than 1×10^7 times of switching,[18] which confirmed the repeatability of the dipole switching and the possibility of using this material for some real applications in the field of memory devices. All these facts inspired us to

Prof. X. Chen, Dr. L. Zhang, Prof. Z. L. Wang
Beijing Institute of Nanoenergy and Nanosystems
Chinese Academy of Sciences
Beijing 100083, China
E-mail: zhong.wang@mse.gatech.edu
Prof. M. Iwamoto, Z. Shi
Department of Physical Electronics
Tokyo Institute of Technology
2-12-1 S3-33 O-okayama
Meguro-ku, Tokyo 152-8552, Japan
Prof. Z. L. Wang
School of Materials Science and Engineering
Georgia Institute of Technology
Atlanta, Georgia 30332–0245, USA

DOI: 10.1002/adfm.201403577

© 2014 WILEY-VCH Verlag GmbH & Co. KGaA, Weinheim

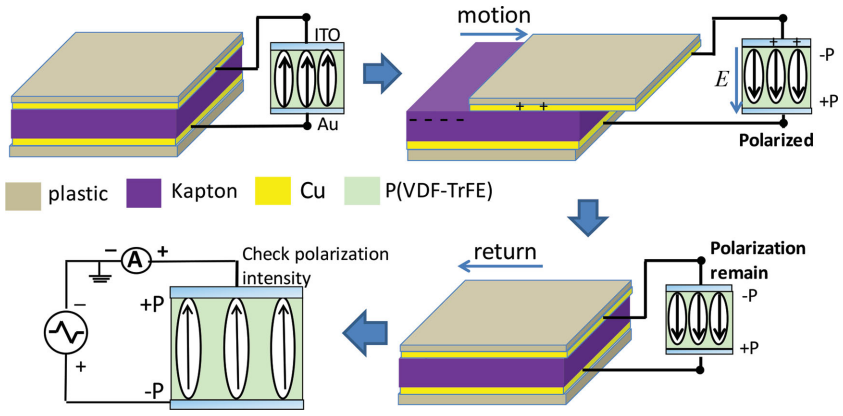

Figure 1. Sketch of the device structure and four steps working principle of the memory system based on sliding TENG and the P(VDF-TrFE) sample.

couple P(VDF-TrFE) thin film and TENG for realizing an effective and self-powered memory system to record mechanical displacement.

In this study, we demonstrated a new application of TENG as a self-powered memory system based on two kinds of TENGs (sliding mode and single-electrode mode) and a P(VDF-TrFE) thin film. With the tribo-electrification facilitated by sliding friction, the changing of the contact area between two surfaces leads to a voltage output applied to the P(VDF-TrFE) thin film. Accordingly, the dipole moment inside the P(VDF-TrFE) thin film is polarized and the polarization intensity can be considered as the memorized information corresponding to the motion of the TENG. Given this working principle, the minimum area changing of 30 mm^2 can be recorded in the P(VDF-TrFE) thin film. By using sliding TENG, we systematically studied the influence of the sliding parameters (the displacement, the duration time, and the velocity) on the memory effect, which illuminates the reliable and stable capability of this work principle. By fabricating a single-electrode TENG matrix, we also demonstrated the trace memorization in two-dimensional (2D) space. This work will open up an application of TENGs with monitoring and memorizing different types of naturally existing mechanical displacements.

2. Results and Discussion

2.1. Memory System with Sliding Mode TENG

Figure 1 illustrates a schematic diagram of the fabricated memory system for realizing the memory effect for the one-dimensional (1D) mechanical displacement, which consists of a sliding mode TENG prototype connected to a P(VDF-TrFE) thin film sample. The sliding TENG employed here is similar to the previous report.[19] The P(VDF-TrFE) thin film sample is consisted of indium tin oxides (ITO)/P(VDF-TrFE)/Au, which shows a metal–insulator–metal (MIM) structure. The detailed fabrication process is described in the Experimental Section. The working principle of this memory system was also depicted in the schematic diagram of Figure 1. The whole process can be divided into four steps. First, the MIM sample of P(VDF-TrFE) was connected to the output electrodes of a sliding mode TENG and the dipole moments inside the MIM sample were pointed in the opposite direction with respect to the output voltage signal from the TENG. Second, the top plate of the TENG slides for a distance and accordingly an electric field was applied to the P(VDF-TrFE) MIM sample due to the tribo-electrification process. With the applied electric field, the dipole moments inside the MIM sample were polarized and switched to a different direction, where the polarization intensity depended on the magnitude of the applied electric field, namely, the sliding distance of TENG. After that, the TENG can return to the original position, while the polarization of the MIM sample remains due to the ferroelectric behavior of P(VDF-TrFE)[20,21] and the information of the mechanical motion was stored inside the P(VDF-TrFE) MIM sample. Finally, another computed power source can be applied to the P(VDF-TrFE) sample for measuring the polarization of the dipole moments and therefore we can read the memorized information during and after the sliding motion of the TENG.

In our experiment, the polarization intensity of ferroelectric P(VDF-TrFE) thin film was measured by using the conventional displacement current measurement (DCM), which offered us a simple way to read the memorize information inside the thin film. In the DCM, a ramp voltage was generated from a function generator and was then applied onto the ITO electrode of the MIM sample with respect to the Au electrode (see Figure 1). An electrometer (Keithley 6517) and a digital multimeter (Keithley 2000) were utilized to record the current–voltage (I–V) characteristics.

The total current flowing through the ITO/P(VDF-TrFE)/Au sample was the sum of the conduction current and displacement current, but the displacement current dominantly flew in our MIM sample because of the good electrical insulating property of the P(VDF-TrFE) layer. Note that the origins of displacement current are electrode charging, accumulation of charges at layer interfaces, and dipolar turn-over in the P(VDF-TrFE) layer. The dipolar turn-over occurred when the electric field across the P(VDF-TrFE) layer reached the coercive field $E_c = 0.4$ MV cm^{-1}.[22] Briefly, the DCM in our case can be given as[14,15]

$$I = \left(C\frac{\partial V}{\partial t} + \frac{\partial P}{\partial t} \right) S \quad (1)$$

Here, C is the capacitance of P(VDF-TrFE) layer and P is the remnant polarization density of P(VDF-TrFE) layer, which is defined as positive when dipoles point in upward orientation, as illustrated in the final step of Figure 1. In Equation (1), the first part is related to the charging of the electrode, which is determined by the frequency of the applied voltage, and the second part is related to the switching of the dipole moment, which can provide the information of polarization intensity. The typical results from the DCM experiment can be found in **Figure 2**a, where two current peaks can be clearly observed

© 2014 WILEY-VCH Verlag GmbH & Co. KGaA, Weinheim
Adv. Funct. Mater. **2014**,
DOI: 10.1002/adfm.201403577

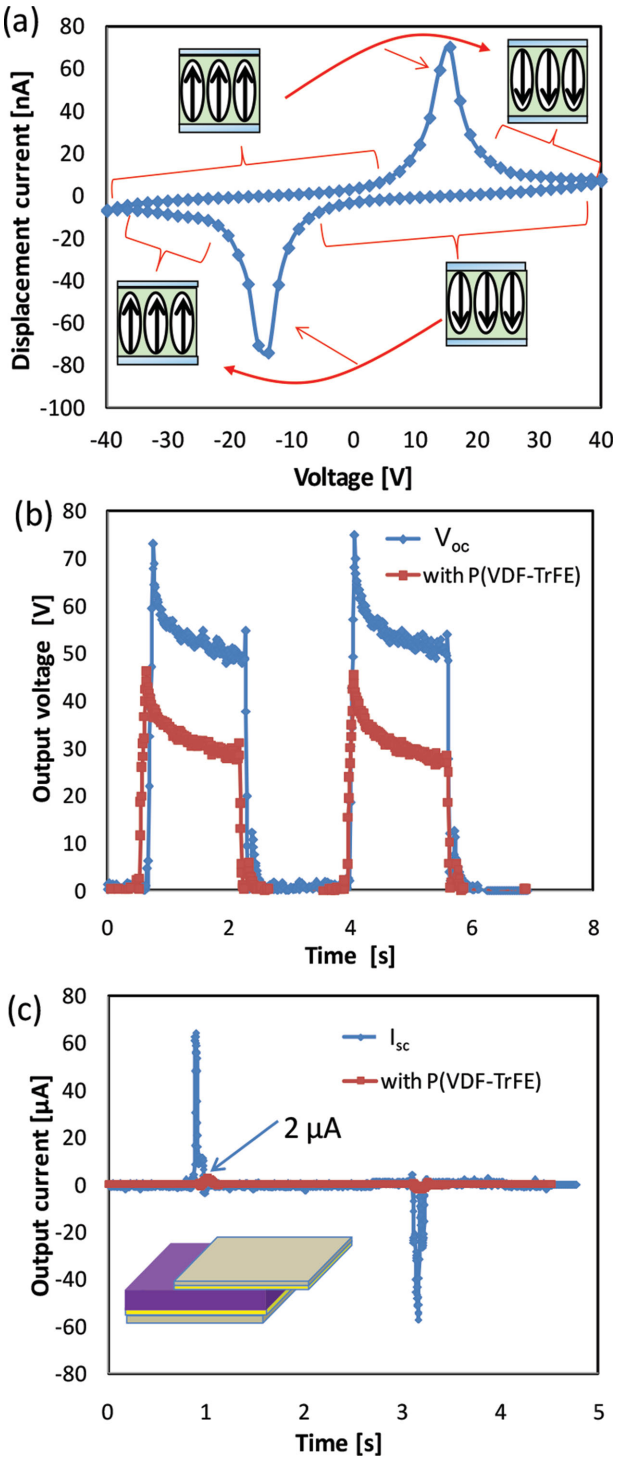

Figure 2. a) The DCM results of the P(VDF-TrFE) MIM sample with the ramp voltage from –25 to 25 V (double circulation). b) The output voltage of sliding mode TENG under open-circuit condition and with the P(VDF-TrFE) applied as a load. c) The output current of sliding mode TENG under short-circuit condition and with P(VDF-TrFE) sample.

from the I–V curve. (The voltage amplitude V_m is 40 V.) As can be seen in Equation (1), the current peak in Figure 2a was caused by the switching (turn-over) of the dipole moment in P(VDF-TrFE).[14,15] In Figure 2a, two peaks were generated at 15.8 V in the process $0 \rightarrow V_m$ and at –15.8 V in the process $0 \rightarrow -V_m$. Meanwhile, by integrating the peak area in Figure 2a, the saturated polarization density was calculated to be $\Delta P = 17.6\ \mu C\ cm^{-2}$. The polarization of the P(VDF-TrFE) depends on the amplitude and the duration time of the applied voltage signal.[22,23] After P(VDF-TrFE) thin film was polarized by the sliding TENG, a ramp voltage signal with the opposite direction with respect to the polarity of the dipole (from 0 to V_m or from 0 to $-V_m$, depending on the polarity of the P(VDF-TrFE)) was applied to the P(VDF-TrFE) sample and such applied voltage would turn over all the dipole that was prepolarized by the sliding TENG. Hence, the induced current peak during this process characterized the recorded information, where both the peak position and the peak area need to be considered (see Figure 1).

The electrical output of the prepared sliding TENG was measured with the top plate guided by a linear motor in the direction parallel to the long-edge of the bottom plates. At the beginning, two plates are aligned with each other and the maximum sliding displacement of top plate was 8 cm, which was determined by the moving extent of the linear motor. The sliding movement was in a symmetric acceleration–deceleration mode with an acceleration rate of $\pm 20\ m\ s^{-2}$. The open-circuit voltage (V_{OC}) was measured by an electrometer with a very large input resistance. The copper foil at the inner side of the top plate is chosen as the positive electrode and later it will be connected to the ITO electrode of the MIM sample, while the electrode at the back of Kapton film was connected to the Au electrode from P(VDF-TrFE) sample. When the plates in the TENG slide from the contact position to the maximum separated position (8 cm) under a speed of $1\ m\ s^{-1}$, the V_{OC} jumped from 0 to ≈75 V (Figure 2b), which reflects the induced potential difference between the two electrodes by the in-plane charge separation. It is important to note that if the output voltage of TENG is too high, the P(VDF-TrFE) thin film may be broken down. In that case, we need to increase the film thickness of the P(VDF-TrFE). Meanwhile, for the TENG connected to the P(VDF-TrFE) sample, the output voltage at the same separation position decreased to 48 V (Figure 2b). At the separation position, the V_{OC} decayed a little bit due to the slow charge leakage through the electrometer and the charge relaxation on the tribo-surface.[19] When the TENG slid back to the original position, the voltage signal jumped back to 0. The output current was also measured at both the short-circuit condition (I_{SC}) and the condition with the P(VDF-TrFE) sample. As shown in Figure 2c, the current was measured to be about 60 μA under a maximum sliding velocity of $1\ m\ s^{-1}$. However, when the TENG was connected to MIM sample, the output current was decreased to 2 μA, which was due to the good insulating performance of the P(VDF-TrFE).

First, we will use the P(VDF-TrFE) sample to memorize the different displacements of the TENG. At the beginning, the P(VDF-TrFE) MIM sample was polarized by using stable power source and then connected to the output end of TENG. The orientation of the dipole moment inside the MIM sample was in the opposite direction with the output voltage of TENG, so that the MIM sample can be reversely polarized by the output voltage from TENG. The top plate of TENG moved to a certain

© 2014 WILEY-VCH Verlag GmbH & Co. KGaA, Weinheim

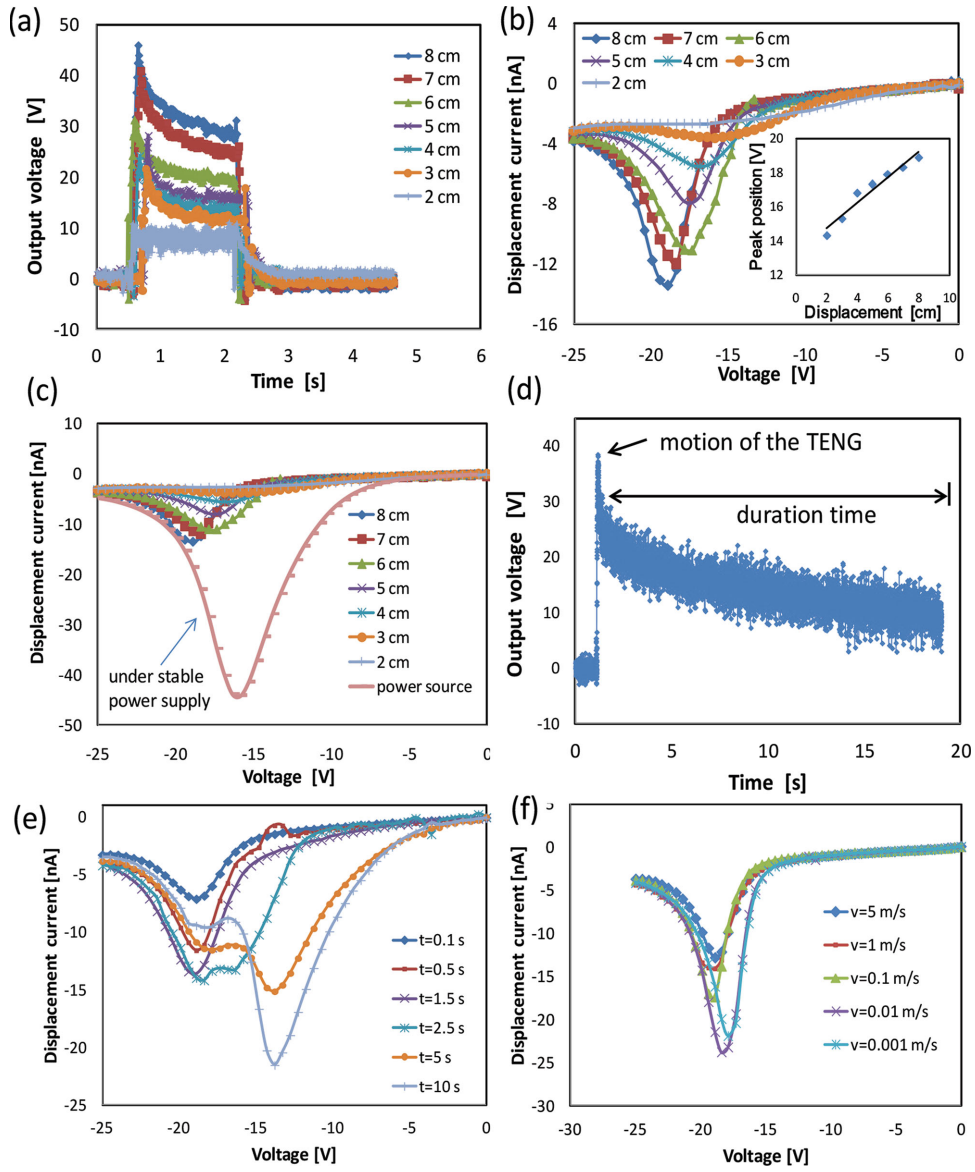

Figure 3. a) The output voltage of the TENG with different sliding distance. b) The change of peak area and peak position from DCM results under different displacement, the inset is the relationship between displacement and displacement current peak postions. c) The DCM results of the current peak induced by TENG and induced by a stable external applied power source. d) The degradation of the output voltage from TENG (displacement 80 mm, velocity 1 m s^{-1}). e) The DCM results of P(VDF-TrFE) sample under different duration time. f) The DCM results of P(VDF-TrFE) sample with different volocity of the TENG.

distance and then returned to its original position. Accordingly, a voltage pulse signal was generated, as shown in Figure 2b, and such pulse signal was recorded by the P(VDF-TrFE) due to the ferroelectric performance. As illustrated in **Figure 3**a, when the sliding distance changed from 2 to 8 cm, the output voltage increased monotonically with the displacement. The output voltage is decided by the induced surface charge density during the tribo-motion and it is also influenced by the capacitance changing between two electrodes. In previous research, the detailed analysis of this variation process has been offered.[24] By neglecting the leakage current through the insulating MIM sample, a simple calculation for the output voltage can be given as

$$V = \frac{Q}{C} = \frac{\sigma \Delta S}{C_T + C_P} \quad (2)$$

Here, the σ is the surface charge density due to tribo-electrification, ΔS is the change of contact area, C_T is the capacitance value of the overlapped region of TENG, which also changes with the displacement, and C_P is the capacitance of P(VDF-TrFE) film. The motion velocity was fixed at 1 m s^{-1} and the duration time during the forward and backward motion was 1.5 s. For each displacement, TENG was stopped after one motion cycle and thus only one voltage pulse was applied to the P(VDF-TrFE) sample. Meanwhile, the memorized polarization intensity can be resolved from the DCM experiment, as can be seen

© 2014 WILEY-VCH Verlag GmbH & Co. KGaA, Weinheim
Adv. Funct. Mater. **2014**,
DOI: 10.1002/adfm.201403577

in Figure 3b. In the DCM experiment, a ramp voltage signal (0 to −25 V) was applied to the MIM sample, since the TENG provided positive output voltage to the MIM sample. In Figure 3b, the current peak was related to the switching of the dipole inside the P(VDF-TrFE) MIM sample. With the decrease of the sliding distance, the areas of induced current peak in the DCM experiments were also decreased (see Figure 3b). Finally, when the sliding distance was decreased to be 2 cm, the current peak in DCM result was nearly disappeared. Hence, the DCM results from Figure 3b demonstrated that P(VDF-TrFE) thin film is able to memorize the sliding displacement of TENG. On the other hand, it can be found that the peak position of DCM results also shifted with the changing of the sliding distance, as can be seen in Figure 3b. This result suggested that P(VDF-TrFE) sample has a promising capability to not only detect the motion of the TENG but also memorize the detailed displacement distances. As can be seen in the insert of Figure 3b, the peak position of the DCM results shifted almost linearly with the motion distance and the DCM results can help us to distinguish different displacement distance with a minimum resolution of 1 cm. These results confirmed the possibility of this memory system for recording the detailed 1D mechanical displacement and no external power supply is needed due to the self-powered capability of TENG. The reason why the shift of the peak position happens can be explained based on the results in Figure 3c. As shown in Figure 3c, the DCM results under the stable voltage source exhibited a large current peak and all of the peaks generated by TENG output were included in the large peak area. Hence, we know that P(VDF-TrFE) thin film can only be partially polarized by TENG output. For a large displacement case, the output voltage from TENG was higher and therefore the "high energy" dipole molecules inside the P(VDF-TrFE) thin film, which can only be switched by a high external electric field, would be preferentially influenced by this voltage signal. The shift of the current peak in accordance with different displacement has been confirmed by repeating the experiments with different samples. However, the detailed reasons why the "high energy" dipoles are preferentially influenced by high voltage signal still need further analysis in the future study. When the displacement of TENG was decreased, the output voltage was also decreased and accordingly those "high energy" dipoles cannot be influenced by this voltage signal, which lead to the shift of the current peak to the low voltage region. It is interesting to note that for most of TENG structure, the moving displacement is usually in proportion to the output voltage, which suggests that P(VDF-TrFE) is suitable to memorize the detailed displacement for all these TENG devices. More importantly, the dipole polarization usually can remain unchanged inside the P(VDF-TrFE) sample for more than two weeks.[25] We have also tested the degradation of the dipole polarity in room temperature and no significant degradation was observed after more than 7 days, which proved the reliability of such memory device.

In order to further study the sensitivity of this memory system, we selected several parameters of TENG to clarify their contributions to the polarization of the dipole moment in P(VDF-TrFE) sample. The polarization of P(VDF-TrFE) thin film is decided by the amplitude and the duration time of the applied voltage signal. With the decrease of the voltage amplitude, the duration time should be increased accordingly.[17] Hence, it is necessary to study the effect of the duration time of TENG on the memory effect of P(VDF-TrFE) thin film. When the top plate of TENG was stopped at the separation position, the output voltage will gradually decay with time (as illustrated in Figure 3d), due to the slow charge leakage through the P(VDF-TrFE). The results in Figure 3d showed the degradation of the voltage on P(VDF-TrFE) sample during duration time of the linear motor, and the charge dissipation mechanism of this process is quite an interesting topic. Usually for the sliding TENG connected to a fixed resistance, the output voltage will be a fix value and show slight degradation with time. However, the P(VDF-TrFE) thin film with the thickness of 350 nm does not have extremely good insulating performance, which means leakage current flows through the sample and the insulating performance of the sample may decrease with time. Another possible charge dissipation mechanism may be related to the switching of the dipoles. Knowing that the measured voltage on the P(VDF-TrFE) sample is the sum of the external voltage (applied from TENG) and the internal potential drop (induced by the dipole polarization). With the increase of retention time, dipoles are gradually polarized and switched to a different direction. The dipole polarization leads to the change of the total potential drop across the sample. Meanwhile, the humidity and temperature are both important factor related to this process. However, the sample was sealed with dry agent and thus we did not consider the influence from humidity. The further study related to this factor is still necessary. Until the voltage signal is decreased to be smaller than the coercive electric field for dipole switching, the polarization of the MIM sample will continue. At the meantime, the polarization intensity of the P(VDF-TrFE) sample under different duration time was also studied, as can be seen in Figure 3e. (Here the motion distance is 8 cm and velocity is 1 m s^{-1}.) With the increase of duration time, the peak area of DCM results increased significantly, indicating that we can enhance the resolution of the memory effect by extending the duration time for each motion cycle. It is also important to point out that a short duration time is not the fatal problem for this memory system. For the duration time smaller than 0.1 s, P(VDF-TrFE) sample still can clearly memorize the motion of TENG, since the common switching time for a dipole is in the scale of 10^{-5} s.[17] The velocity of the sliding plate is another important parameter for TENG. The memorized DCM signal along with different sliding velocity was concluded in Figure 3f. With the decrease of the velocity, the time for polarization was increased accordingly and therefore polarization will show small increase (see Figure 3f). Knowing that the polarization of P(VDF-TrFE) is determined by the applied voltage and has less interaction with the conduction current, the high velocity of TENG will have no contribution to enhance the memory effect. However, if the velocity was too slow (<0.001 m s^{-1}), the leakage current and the relaxation of induced charges started to suppress the output voltage, which resulted in the decrease of the peak area. Through the sensitivity experiment, we found that this memory system can work stably within the velocity range from 0.001 to 5 m s^{-1},

© 2014 WILEY-VCH Verlag GmbH & Co. KGaA, Weinheim

while the duration time can be varied from 0.1 to 10 s, which confirmed its promising application as a self-powered memory device.

As can be seen in Figure 3b, the resolution of this memory system is in the scale of centimeter, which is due to the low output voltage provided by this sliding TENG. In fact, the resolution of this memory system is not determined by the displacement of the sliding motion but by the output voltage that can be generated from the TENG. As can be seen in Figure 2a,b, any tribo-motion that can generate an output voltage larger than 10 V will be recorded by this memory system (this voltage value is decided by the thickness of P(VDF-TrFE)), which is a quite easy task according to the output characteristic of the TENG.[1–5] Hence, the resolution of this memory system can be further improved by optimizing the structure and the output of TENG. Consequently, at a velocity of 1 m s^{-1}, the polymer thin film with a size of 3.1 mm^2 is possible to memorize a minimum displacement of 5 mm ($\Delta S = 200$ mm^2) at a distance resolution of 5 mm. The detailed results can be seen in the Supporting Information. On the other hand, the output characteristic of the sliding mode TENG also indicates that it cannot achieve high output voltage with small displacement.[24] For the sliding TENG, the capacitance value (C_T) between two output electrodes is decided by the overlapped region between two plates. If the displacement is small, the overlapped region will be large and C_T will be increased, which leads to the suppression of the output voltage (see Equation (2). In order to memorize the motion in small scale, it is better to use some different type of TENG, for example, the single-electrode TENG.

2.2. Memory System with Single-Electrode TENG Matrix

The memory system based on the sliding TENG and the P(VDF-TrFE) thin film can only record the 1D displacement, and in order to fully demonstrate the capability of this memorization method, it is necessary for us to design a memory system to retrieve the 2D motion trace. Therefore, we prepared a self-powered sensor matrix based on the working principle of single-electrode TENG[26] to work with the P(VDF-TrFE) thin film for monitoring 2D movements. As shown in **Figure 4**a,b, the single-electrode TENG matrix was composed of two main components, a 50 μm-thick layer of Kapton at the bottom of the moving object and patterns of 100 μm-thick Al films at the surface of a flat acrylic glass. Each Al film served as an electrode of the single-electrode TENG and an individual P(VDF-TrFE) MIM sample was connected between each Al electrode and the ground for recording the output signal (see Figure 4a). The photographs of fabricated TENG matrix as well as electrodes with different size were presented in Figure 4c. The flat plate made by acrylic glass had a device area of 60 × 60 mm. Each square Al electrode in the 4 × 4 matrix pattern had a side length of 6 mm, and the gap between two adjacent Al electrodes was also 6 mm.

The working principle of this 2D memory system was shown in Figure 4a. An object with the Kapton film on the bottom surface was moving towards the Al electrode. In the original position, the negative charges were distributed on the surface of Kapton as a result of tribo-electrification after a contact with previous Al. When the Kapton approaches the Al electrode, the negative charge on the Kapton surface resulted in a potential

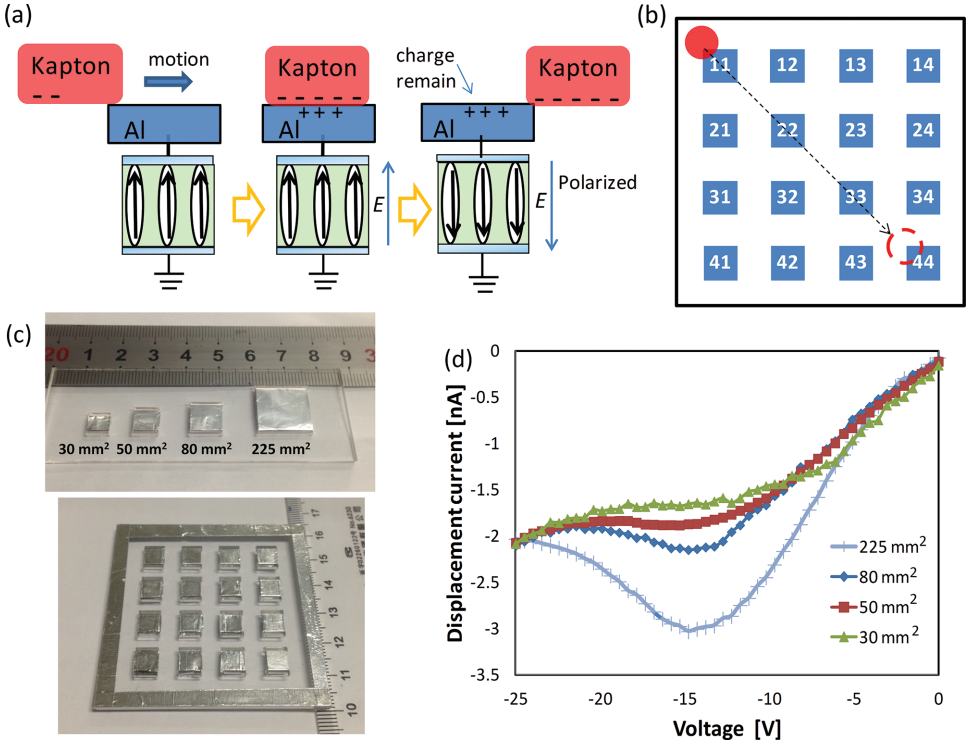

Figure 4. a) Sketch of the device structure and working principle of the memory system based on single-electrode TENG and P(VDF-TrFE) sample. b) The sketch of fabricated 4 × 4 TENG matrix for decting the 2D motion. c) Photograph of electrodes with different sizes and the TENG matrix with 4 × 4 pixels in size of 6 mm × 6 mm. d) The DCM results of P(VDF-TrFE) sample connected to electrodes with different sizes.

© 2014 WILEY-VCH Verlag GmbH & Co. KGaA, Weinheim
Adv. Funct. Mater. **2014**,
DOI: 10.1002/adfm.201403577

difference between Al electrode and the ground. However, this potential drop will not influence the dipole orientation in the P(VDF-TrFE) because the dipoles have already been polarized in the same direction. When Kapton film totally overlapped Al electrode, positive charges were induced on the surface of Al due to contact electrification. Later, once the top Kapton slid outward, it resulted in the residual of the induced positive charges on the Al and accordingly a potential drop between Al electrode and the ground was established. This potential drop was in the opposite direction with the dipole orientation in the P(VDF-TrFE) thin film and thus the P(VDF-TrFE) can be polarized. Finally, by using DCM, the recorded polarization intensity can be obtained and we can retrieve the trace of the moving object.

In comparison with sliding TENG, the output voltage of such single-electrode TENG is only determined by the capacitance value of the P(VDF-TrFE)

$$V = \frac{Q}{C} = \frac{\sigma \Delta S}{C_P} \tag{3}$$

and the duration time for each electrode can be considered as infinite large. (The Kapton object will not move back.) Hence, it is possible to obtain higher displacement resolution with this single-electrode TENG. As can be seen in Figure 4c, we prepared four kinds of Al electrodes with the area size varied from 225 to 30 mm^2. After the Kapton slid across all these electrodes, the memorized information was read by DCM experiment, as shown in Figure 4d. Here, we confirmed that the minimum area changing for this memory system is about ΔS = 30 mm^2, which is more than 6 times smaller than the value from sliding mode TENG. This value may still be further enhanced if we apply some surface etching treatment or nano imprint lithography technique to increase the effective surface area of the tribo-layer.[9,26] On the other hand, if we want to memorize some extremely high speed motion, the single electrode TENG can be a better solution in comparison with sliding-mode TENG. After the moving object moves across the surface of the electrode, it will not return to the same electrode. Hence the retention time can be considered as infinite large. This working mechanism can be applied for the very high speed motion's case.

In order to practically demonstrate the memory system's response to a motion, the Kapton object was slid across the top surface of the TENG matrix and the TENG matrix was fixed on the platform to generate the outputs (see Figure S2, Supporting Information). The P(VDF-TrFE) samples were utilized to memorize the output signals from each electrode separately. In the sliding TENG's case, we already proved that the P(VDF-TrFE) sample can work stably within the motion

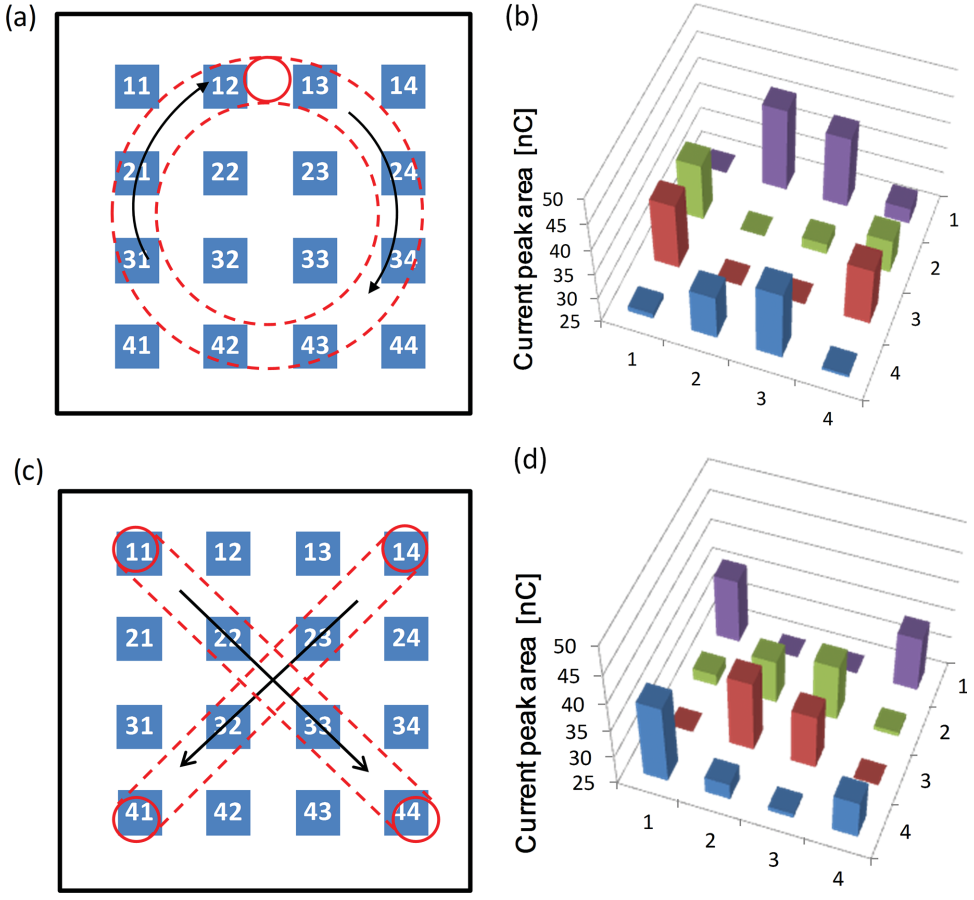

Figure 5. a) Illustration of the Kapton moving along a path of letter "O." b) The calculated current peak area for each P(VDF-TrFE) sample in response to the motion trajectory of letter "O." c) Illustration of the Kapton moving along a path of letter "X." d) The calculated current peak area for each P(VDF-TrFE) sample in response to the motion trajectory of letter "X."

© 2014 WILEY-VCH Verlag GmbH & Co. KGaA, Weinheim

velocity ranged from 0.001 to 5 m s^{-1}. Hence, in this experiment, the Kapton object is moved by human hands with an approximate velocity of 0.1 m s^{-1}. As exhibited in **Figure 5**, when the Kapton film moved on the TENG matrix along the path of letter "O:" electrode 13 (E13) → electrode 24 (E24) → electrode 34 (E34) → electrode 44 (E44) → electrode 42 (E42) → electrode 31 (E31) → electrode 21 (E21) → electrode 12 (E12) (Figure 5a), the generated triboelectric signal can be recorded by the P(VDF-TrFE) samples connected to each electrode. Then, the DCM experiment was applied to read the recorded information in the P(VDF-TrFE) samples. The current peak area of DCM results can be integrated in time domain and this integrated value is the transported charges across the sample (current peak area).[20,21] The switching of the dipole results in the current peak in the DCM (see Figure 2a) and the integration of the current peak area can illustrate the intensity of the dipole switching. Hence, after drawing a letter "O" on the surface of TENG matrix (see Figure 5a), the memorized information in each P(VDF-TrFE) sample was calculated by integrating the current peak area and the results were concluded in Figure 5b. As illustrated in Figure 5b, the P(VDF-TrFE) samples related to the motion trajectory clearly possessed higher current peak area, which proved the possibility of trace memorization using this method. Then, another moving trajectory of a letter "X" was also performed on the surface of the TENG matrix, as shown in Figure 5c. Accordingly, the calculated peak areas from each P(VDF-TrFE) sample were summarized in Figure 5d and the results were in good agreements with the motion trajectory.

3. Conclusions

In summary, by coupling P(VDF-TrFE) MIM sample with both the sliding TENG and the single-electrode TENG matrix, we have demonstrated a novel self-powered memory system to memorize the motion in both 1D and 2D spaces. This memory system can record the detailed displacement distance of a sliding TENG and it can also retrieve the motion trace on the surface of the single-electrode TENG matrix. The P(VDF-TrFE) MIM sample with the size of 3.1 mm^2 can memorize a minimum area changing of 30 mm^2, while it can also work stably within the velocity range from 0.001 to 5 m s^{-1}. The similar working principle of this memory system can be applied to other type TENGs, liking rotating TENG, contact TENG, and so on. The good stability and repeatability of the P(VDF-TrFE) thin film guaranteed the promising application of such memory technique for monitoring various mechanical motions. Furthermore, the flexibility of the P(VDF-TrFE) polymer can also open some possible application in the field of flexible electronics. Together with the self-powered capability of TENG, this memory system could potentially be used as a self-powered memory disk for electronic skin or some other soft electronics devices.

4. Experimental Section

Fabrication of Sliding Mode TENG: The sliding mode TENG is structurally composed of two plates (150 × 80 mm) with plastic slides as the supporting substrates to ensure the surface flatness (Figure 1a). The copper foil with rectangular shape (150 × 40 mm) was printed on the surface of the both sliding plates by using printed circuit broad technique, where the foil plays dual roles of a triboelectric surface and two electrodes. The Kapton adhesive tapes (thickness ≈ 100 μm) are purposely chosen as the triboelectric layers adhered on surface of one plate (copper foil is overlapped by the Kapton tape). The two plates are kept in parallel with each other, where the inner surfaces are in intimate contact. The bottom plate with the Kapton tape was fixed to a stationary stage, whereas the top plate with only copper foil slides against the bottom one. During the sliding motion, the contact area changes periodically by the mechanical motion along the long-edge of the plates. By employing a numerical control linear motor to drive the top plate, we can precisely regulate the speed and the moving distance of the sliding-plate.

Fabrication of P(VDF-TrFE) Thin Film: The P(VDF-TrFE) copolymer (72/28, mol%) was first dissolved in methyl-ethyl-ketone solvent and then directly spin-coated onto a pre-cleaned ITO substrate, followed by an annealing at 150 °C for 1.5 h in dry nitrogen atmosphere. The thickness of the P(VDF-TrFE) layer was determined around 350 nm by using a profilometer. If we change the concentration of the P(VDF-TrFE) solution for spin-coating, the film thickness can be changed.[21] An Au electrode with the thickness of 100 nm was evaporated onto the annealed P(VDF-TrFE) thin film. The device area was around $S = 3.1$ mm^2. A prepared MIM sample was sealed with a dry agent to avoid degradation during the measurements.

Supporting Information

Supporting Information is available from the Wiley Online Library or from the author.

Acknowledgements

The authors thank for the support from the "thousands talents" program for pioneer researcher and his innovation team, China, National Natural Science Foundation of China (Grant No. 51432005), and Beijing City Committee of science and technology (Grant Nos. Z131100006013004 and Z131100006013005).

Received: October 14, 2014
Revised: November 10, 2014
Published online:

[1] F.-R. Fan, Z.-Q. Tian, Z. L. Wang, *Nano Energy* **2012**, *1*, 328.
[2] Z. L. Wang, *ACS Nano* **2013**, *7*, 9533.
[3] G. Zhu, J. Chen, Y. Liu, P. Bai, Y. S. Zhou, Q. S. Jing, C. F. Pan, Z. L. Wang, *Nano Lett.* **2013**, *13*, 2282.
[4] L. Zheng, Z. H. Lin, G. Cheng, W. Wu, X. Wen, S. Lee, Z. L. Wang, *Nano Energy* **2014**, *9*, 291.
[5] Y. Yang, G. Zhu, H. Zhang, J. Chen, X. Zhong, Z.-H. Lin, Y. Su, P. Bai, X. Wen, Z. L. Wang, *ACS Nano* **2013**, *7*, 94618.
[6] H. L. Zhang, Y. Yang, Y. J. Su, J. Chen, C. G. Hu, Z. K. Wu, Y. Liu, C. P. Wong, Y. Bando, Z. L. Wang, *Nano Energy* **2013**, *2*, 693.
[7] S. Lee, R. Hinchet, Y. Lee, Y. Yang, Z. H. Lin, G. Ardila, L. Montes, M. Mouis, Z. L. Wang, *Adv. Funct. Mater.* **2014**, *24*, 1163.
[8] Y. F. Hu, C. Xu, Y. Zhang, L. Lin, R. L. Snyder, Z. L. Wang, *Adv. Mater.* **2011**, *23*, 4068.
[9] G. Zhu, Y. S. Zhou, P. Bai, X. S. Meng, Q. Jing, J. Chen, Z. L. Wang, *Adv. Mater.* **2014**, *26*, 3788.
[10] Y. Xie, S. Wang, S. Niu, L. Lin, Q. Jing, J. Yang, Z. Wu, Z. L. Wang, *Adv. Mater.* **2014**, DOI: 10.1002/adma.201402428.
[11] J. Yang, J. Chen, Y. Liu, W. Yang, Y. Su, Z. L. Wang, *ACS Nano* **2014**, *8*, 2649.

© 2014 WILEY-VCH Verlag GmbH & Co. KGaA, Weinheim

[12] Y. Xie, S. Wang, S. Niu, L. Lina, Q. Jing, Y. Su, Z. Wu, Z. L. Wang, *Nano Energy* **2014**, *6*, 129.
[13] R. C. G. Naber, C. Tanase, P. W. M. Blom, G. H. Gelinck, A. W. Marsman, F. J. Touwslager, S. Setayesh, D. M. deLeeuw, *Nat. Mater.* **2005**, *4*, 243.
[14] L. Hu, S. Dalgleish, M. M. Matsushita, H. Yoshikawa, K. Awaga, *Nat. Commun.* **2014**, *5*, 3279.
[15] X. Cui, D. Taguchi, T. Manaka, W. Pan, M. Iwamoto, *Org. Electron.* **2014**, *15*, 537.
[16] Y. Yuan, T. J. Reece, P. Sharma, S. Poddar, S Ducharme, A. Gruverman, Y. Yang, J. Huang, *Nat. Mater.* **2011**, *10*, 296.
[17] K. S. Nalwa, J. A. Carr, R. C. Mahadevapuram, H. K. Kodali, S. Bose, Y. Chen, J. W. Petrich, B. Ganapathysubramanian, S. Chaudhary, *Energy Environ. Sci.* **2012**, *5*, 7042.
[18] H. Xu, J. Zhong, X. Liu, J. Chen, D. Shen, *Appl. Phys. Lett.* **2007**, *90*, 092903.
[19] S. Wang, L. Lin, Y. Xie, Q. Jing, S. Niu, Z. L. Wang, *Nano Lett.* **2013**, *13*, 2226.
[20] D. Mao, M. A. Quevedo-Lopez, H. Stiegler, B. E. Gnade, H. N. Alshareef, *Org. Electron.* **2010**, *11*, 925.
[21] X. Chen, W. Ou-Yang, M. Weis, D. Taguchi, T. Manaka, M. Iwamoto, *J. Appl. Phys.* **2010**, *49*, 021601.
[22] F. Xia, H. Xu, F. Fang, B. Razavi, Z.-Y. Cheng, Y. Lu, B. Xu, Q. M. Zhang, *Appl. Phys. Lett.* **2001**, *78*, 1122.
[23] W. Ou-Yang, M. Weis, X. Chen, T. Manaka, M. Iwamoto, *J. Chem. Phys.* **2010**, *131*, 104702.
[24] S. Niu, Y. Liu, S. Wang, L. Lin, Y. S. Zhou, Y. Hu, Z. L. Wang, *Adv. Mater.* **2013**, *25*, 6184.
[25] Y. Yuan, P. Sharma, Z. Xiao, S. Poddar, A. Gruverman, S. Ducharme, J. Huang, *Energy Environ. Sci.* **2012**, *5*, 8558.
[26] Y. Yang, H. Zhang, J. Chen, Q. Jing, Y. S. Zhou, X. Wen, Z. L. Wang, *ACS Nano* **2013**, *7*, 7342.

© 2014 WILEY-VCH Verlag GmbH & Co. KGaA, Weinheim